Quadruply Bonded Dimolybdenum Compounds with Polydentate Phosphines. 1. Mo_2X_4(tetraphos-1) (tetraphos-1 = $Ph_2PCH_2CH_2P(Ph)CH_2CH_2P(Ph)CH_2CH_2PPh_2$, X = Cl, Br), the First Examples of Enantiomeric 1,2,5,8/1,2,6,7 and 1,2,5,7/1,2,6,8 Types

Jhy-Der Chen,† F. Albert Cotton,* and Bo Hong

Department of Chemistry and The Laboratory for Molecular Structure and Bonding, Texas A&M University, College Station, Texas 77843

Received December 16, 1992

Five meso and racemic diastereomers, *rac*-Mo_2Cl_4(tetraphos-1)·CH_2Cl_2 (**1**), *meso*-Mo_2Cl_4(tetraphos-1) (**2**), *rac*-Mo_2Br_4(tetraphos-1)·0.5 CH_2Cl_2 (**3**), *meso*-Mo_2Br_4(tetraphos-1)·CH_2Cl_2 (**4**), and *meso*-Mo_2Br_4(tetraphos-1)·1.5 THF (**5**) (tetraphos-1 = $Ph_2PCH_2CH_2P(Ph)CH_2CH_2P(Ph)CH_2CH_2PPh_2$) have been synthesized and structurally characterized. Among them are two new types of geometrical isomers, namely, 1,2,5,7/1,2,6,8 and 1,2,5,8/1,2,6,7 enantiomeric pairs, of $M_2X_4L_4$ complexes. Four significant differences emerge as we compare the structures of complexes with the meso and racemic ligands: (i) While the two central phosphorus donor atoms coordinate to different Mo centers in the racemic ligand, they coordinate to the same Mo atom in the complex of the meso ligand, thus giving the bischelating/single-bridging coordination mode in the former and the chelating/double-bridging mode in the latter. (ii) The average Mo–Mo bond distances, 2.154 Å and 2.190 Å for racemic and meso diastereomers, respectively, are different by 0.037 Å, but they both fall within the range of the distances established for Mo–Mo quadruple bonds. (iii) The average of the four smallest torsional angles is different: 18.8 and 30.0° for the racemic and meso diastereomers, respectively. (iv) While the racemic diastereomers comprise the 1,2,5,8/1,2,6,7 enantiomers, the meso ones are designated as the 1,2,5,7/1,2,6,8 enantiomers. The crystal structures of **1**–**5** are fully described. Crystallographic data for these complexes are as follows: **1**, $C2/c$ with a = 19.527(6) Å, b = 18.210(2) Å, c = 13.241(2) Å, β = 104.85(2)°, V = 4551(2) Å^3, and Z = 4; **2**, $C2/c$ with a = 26.174(5) Å, b = 20.297(5) Å, c = 16.047(7) Å, β = 100.03(3)°, V = 8395(5) Å^3, and Z = 8; **3**, $C2/c$ with a = 19.563(2) Å, b = 18.317(4) Å, c = 13.354(3) Å, β = 104.22(1)°, V = 4638(2) Å^3, and Z = 4; **4**, $P2_1/c$ with a = 16.444(4) Å, b = 21.335(3) Å, c = 25.882(3) Å, β = 91.20(2)°, V = 9078(3) Å^3, and Z = 8; **5**, $P2_1/c$ with a = 19.920(5) Å, b = 17.818(5) Å, c = 15.999(4) Å, β = 111.27(2)°, V = 5292(5) Å^3, and Z = 4. In addition to the structural data for these complexes, $^{31}P\{^1H\}$ NMR and UV–vis spectroscopy have also been used to characterize the complexes.

Introduction

Complexes containing metal–metal quadruple bonds have been subjected to many studies of their structural and spectroscopic properties[1] since the first recognition of the existence of a quadruple bond[2] between two metal atoms in the mid 1960s. In the overall research effort concerning the behavior of metal–metal bonds, studies of the $Mo_2X_4L_4$ (X = halide, CH_3, NCS, NCO, OC_6F_6, etc; L = neutral phosphine ligands) type of complexes containing quadruple bonds between metal atoms have played a prominent part. Such complexes can be approximately described as an Mo_2 unit within a cubic array of four X ligands and four phosphorus atoms as shown in Figure 1. A number of isomers are possible, and they can be enumerated and designated systematically using a previously defined[3] numbering scheme, in which we ignore distorsions from the eclipsed conformation about the Mo_2 axis. For an $M_2X_4L_4$ molecule the following 10 geometrical isomers can be listed with enantiomeric pairs bracketed together: (1) 1,2,3,4; (2) 1,2,3,5/1,2,3,7; (3) 1,2,3,6; (4) 1,2,3,8; (5) 1,2,5,7/1,2,6,8; (6) 1,2,5,8/1,2,6,7; (7) 1,2,5,6; (8) 1,2,7,8; (9) 1,3,5,7; (10) 1,3,6,8.

So far, examples of only three of these isomers have been observed. Most of the complexes with four separate monophosphines belong to the 1,3,6,8 (10) type due to the steric factor which causes the four bulkier phosphine ligands to avoid adjacent positions.[4] The only exception to date is $Mo_2(OC_6F_5)_4(PMe_3)_4$,[5] which was the first example of a 1,2,7,8 (8) type molecule with monophosphine ligands. When bidentate phosphines (LL) are employed, two isomers, commonly called α and β, of $Mo_2X_4(LL)_2$ type of molecules (Figure 2) can be formed. The α form complexes can be unambiguously classified as 1,2,7,8 (8) type. For the β form complexes, those with average torsional angles less than 45° can be described as the 1,3,5,7 (9) isomers and those with torsional angles greater than 45° can be designated as the 1,3,6,8 (10) isomers.[6] None of the remaining geometrical isomers has yet been obtained.

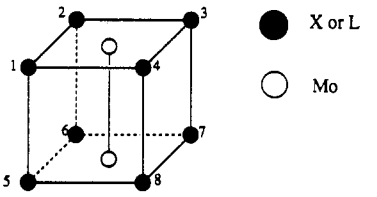

Figure 1. Idealized cubic structure and numbering scheme for $Mo_2^4MoX_4L_4$.

† Currently at National Taiwan University, Taipei, Taiwan.

(1) Cotton, F. A.; Walton, R. A. *Multiple Bonds Between Metal Atoms*, 2nd ed.; Oxford University Press: London, 1993.
(2) Cotton, F. A.; Curtis, N. F.; Harris, C. B.; Johnson, B. F. G.; Lippard, S. J.; Mague, J. T.; Robinson, W. R.; Wood, J. S. *Science*, **1964**, *145*, 1305.
(3) Chen, J.-D.; Cotton, F. A. *Inorg. Chem.* **1991**, *30*, 6.
(4) (a) Cotton, F. A.; Extine, M. W.; Felthouse, T. R.; Kolthammer, B. W. S.; Lay, D. G. *J. Am. Chem. Soc.*, **1981**, *103*, 4040. (b) Hopkins, M. D.; Schaefer, W. P.; Bronikowsi, M. J.; Woodruff, W. H.; Miskowski, V. M.; Dallinger, R. F.; Gray, H. B. *J. Am. Chem. Soc.*, **1987**, *109*, 408.
(5) Cotton, F. A.; Wiesinger, K. J. *Inorg. Chem.*, **1991**, *30*, 750.

0020-1669/93/1332-2343$04.00/0

Table I. Crystallographic Data and Data Collection Parameters for **1–5**

	1	2	3	4	5
chem formula	$Mo_2Cl_4P_4C_{42}H_{42}\cdot CH_2Cl_2$	$Mo_2Cl_4P_4C_{42}H_{42}$	$Mo_2Br_4P_4C_{42}H_{42}\cdot 0.5CH_2Cl_2$	$Mo_2Br_4P_4C_{42}H_{42}\cdot CH_2Cl_2$	$Mo_2Br_4P_4C_{42}H_{42}\cdot 1.5THF$
fw	1089.32	1007.34	1224.69	1267.15	1290.38
space group	$C2/c$	$C2/c$	$C2/c$	$P2_1/c$	$P2_1/c$
a, Å	19.527(6)	26.174(5)	19.563(2)	16.444(4)	19.920(5)
b, Å	18.210(2)	20.297(5)	18.317(4)	21.335(3)	17.818(5)
c, Å	13.241(2)	16.047(7)	13.354(3)	25.882(3)	15.999(4)
α, deg	(90)	(90)	(90)	(90)	(90)
β, deg	104.85(2)	100.03(3)	104.22(1)	91.20(2)	111.27(2)
γ, deg	(90)	(90)	(90)	(90)	(90)
V, Å^3	4551(2)	8395(5)	4638(2)	9078(3)	5292(5)
Z	4	8	4	8	4
T, °C	20 ± 1	−60 ± 1	−60 ± 1	20 ± 1	20 ± 1
λ, Å	0.710 73	0.710 73	0.710 73	0.710 73	0.710 73
ρ_{calcd}, g cm^{-3}	1.59	1.589	1.814	1.790	1.620
μ(Mo Kα), cm^{-1}	10.63	10.21	45.55	44.95	38.22
data collcn instrum	CAD-4S	CAD-4S	CAD-4S	Syntex P3	Syntex P3
transmission coefficient	1.00–0.93	0.999–0.677	0.997–0.445	0.999–0.667	0.999–0.940
R,[a] R_w[b]	0.0390, 0.0580	0.0585, 0.0779	0.0468, 0.0657	0.0562, 0.0653	0.04788, 0.06635

[a] $R = \Sigma||F_o| - |F_c||/\Sigma|F_o|$. [b] $R_w = [\Sigma w(|F_o| - |F_c|)^2/\Sigma w|F_o|^2]^{1/2}$; $w = 1/\sigma^2(|F_o|)$.

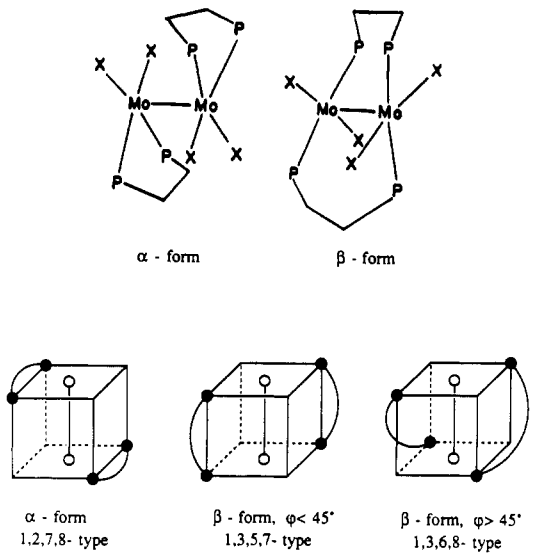

Figure 2. α and β forms of Mo$\equiv$Mo$X_4(LL)_2$ and their isomer types.

In order to overcome the tendency of the larger neutral phosphine ligands to occupy alternate vertices, and thereby to allow the isolation of examples of the remaining isomers, polydentate phosphines containing more than two phosphorus atoms can be chosen to favor or even require such arrangements. Linear tetradentate phosphine ligands are suitable for this purpose since they can both chelate and bridge two metal centers.[7,8] We report here the first examples of two previously unobserved geometrical isomers, namely, the enantiomeric pairs (5) and (6), using the linear tetradentate phosphine ligand tetraphos-1, $Ph_2PCH_2CH_2P^*(Ph)CH_2CH_2P^*(Ph)CH_2CH_2PPh_2$, where the chiral phosphorus atoms are designated by asterisks. Since there are two chiral phosphorus atoms in this ligand, both meso (*R,S* and *S,R*) and racemic (*R,R* and *S,S*) diastereomers exist. Some preliminary results about the synthesis and structure determination of the compound *rac*-Mo_2Cl_4(tetraphos-1)·CH_2Cl_2 (**1**) have been reported in our previous communication.[3]

Table II. Positional and Thermal Parameters for Non-Hydrogen Atoms of *rac*-Mo$\equiv$MoCl$_4$(tetraphos-1)·CH_2Cl_2 (**1**)

atom	x	y	z	B_{eq},[a] Å^2
Mo	0.44783(2)	0.34287(2)	0.19725(3)	1.814(7)
Cl(1)	0.41439(6)	0.21779(6)	0.15316(9)	2.90(2)
Cl(2)	0.46081(6)	0.37297(7)	0.02436(9)	2.94(2)
P(1)	0.36925(6)	0.33248(7)	0.32283(9)	2.27(2)
P(2)	0.40977(6)	0.47288(7)	0.21418(9)	2.42(2)
C(1)	0.2791(2)	0.3098(3)	0.2491(4)	2.7(1)
C(2)	0.2633(3)	0.2363(3)	0.2221(4)	3.7(1)
C(3)	0.1963(3)	0.2177(4)	0.1611(5)	4.5(1)
C(4)	0.1458(3)	0.2700(4)	0.1277(5)	5.0(2)
C(5)	0.1605(3)	0.3430(4)	0.1546(5)	5.0(2)
C(6)	0.2277(3)	0.3625(3)	0.2157(5)	4.0(1)
C(7)	0.3855(2)	0.2671(3)	0.4308(4)	2.7(1)
C(8)	0.4354(3)	0.2133(3)	0.4411(4)	3.7(1)
C(9)	0.4511(3)	0.1675(4)	0.5290(5)	4.6(1)
C(10)	0.4146(4)	0.1783(4)	0.6064(5)	5.1(2)
C(11)	0.3625(4)	0.2318(4)	0.5946(5)	5.4(2)
C(12)	0.3480(3)	0.2761(4)	0.5069(4)	4.4(1)
C(13)	0.3611(3)	0.4207(3)	0.3873(4)	3.5(1)
C(14)	0.5356(3)	0.5543(3)	0.2928(4)	3.5(1)
C(15)	0.3921(3)	0.4864(3)	0.3435(4)	3.7(1)
C(16)	0.3258(2)	0.4931(3)	0.1205(4)	2.8(1)
C(17)	0.2887(3)	0.5573(3)	0.1310(5)	4.1(1)
C(18)	0.2231(3)	0.5693(4)	0.0626(6)	5.3(2)
C(19)	0.1926(3)	0.5188(4)	−0.0142(6)	5.2(2)
C(20)	0.2303(3)	0.4555(4)	−0.0247(5)	4.4(1)
C(21)	0.2962(3)	0.4438(3)	0.0422(4)	3.2(1)
Cl(3)	0.4515(3)	0.0082(3)	0.3061(4)	21.7(2)
C(22)	0.500	0.0582(7)	0.250	14.4(8)

[a] Values for anisotropically refined atoms are given in the form of the equivalent isotropic displacement parameter defined as $^1/_3[a^2a^{*2}B_{11} + b^2b^{*2}B_{22} + c^2c^{*2}B_{33} + 2ab(\cos\gamma)a^*b^*B_{12} + 2ac(\cos\beta)a^*c^*B_{13} + 2bc(\cos\alpha)b^*c^*B_{23}]$.

Experimental Procedures

General Data. All manipulations were carried out under an atmosphere of argon unless otherwise specified. Standard Schlenk and vacuum line techniques were used. Commercial grade solvents were dried and deoxygenated by refluxing at least 24 h over the appropriate reagents and freshly distilled before use. THF, benzene, diethyl ether, and *n*-hexane were purified by distillation from potassium/sodium benzophenone ketyl, dichloromethane was purified by distillation from phosphorus pentoxide, and methanol was purified by distillation from Mg, prior to use.

The tetraphos-1 ligand (as a mixture of diastereomers) was purchased from Strem Chemicals and used as received. Trimethylchlorosilane and

(6) (a) Cotton, F. A.; Falvello, L. R.; Harwood, W. S.; Powell, G. L.; Walton, R. A. *Inorg. Chem.* **1986**, *25*, 3949. (b) Campbell, F. L., III; Cotton, F. A.; Powell, G. L. *Inorg. Chem.*, **1985**, *24*, 177. (c) Campbell, F. L., III; Cotton, F. A.; Powell, G. L. *Inorg. Chem.*, **1985**, *24*, 4384. (d) Agaskar, P. A.; Cotton, F. A. *Inorg. Chem.*, **1986**, *25*, 15. (e) Cotton, F. A.; Dunbar, K. R.; Matusz, M. *Inorg. Chem.*, **1986**, *25*, 3641. (f) Bakir, M.; Cotton, F. A.; Falvello, L. R.; Simpson, C. Q.; Walton, R. A. *Inorg. Chem.* **1988**, *27*, 4197. (g) Campbell, F. L., III; Cotton, F. A.; Powell, G. L. *Inorg. Chem.*, **1984**, *23*, 4222. (h) Chen, J.-D.; Cotton, F. A.; Falvello, L. R. *J. Am. Chem. Soc.* **1990**, *112*, 1076. (i) Chen, J.-D.; Cotton, F. A. *Inorg. Chem.* **1990**, *29*, 1979.
(7) (a) Lanemen, S. A.; Fronczek, F. R.; Stanley, G. G. *Inorg. Chem.* **1989**, *28*, 1207. (b) Laneman, S. A.; Fronczek, F. R.; Stanley, G. G. *Inorg. Chem.* **1989**, *28*, 1872.
(8) Cotton, F. A.; Hong, B. *Prog. Inorg. Chem.* **1992**, *40*, 179.

Table III. Positional and Thermal Parameters for Non-Hydrogen Atoms of *meso*-Mo_2Cl_4(tetraphos-1) (**2**)

atom	x	y	z	B_{eq},[a] Å^2
Mo(1)	0.68259(3)	0.60876(4)	0.31001(4)	1.41(1)
Mo(2)	0.76092(3)	0.57652(4)	0.29948(4)	1.44(1)
Cl(1)	0.67914(8)	0.6697(1)	0.4380(1)	1.95(4)
Cl(2)	0.78417(8)	0.6308(1)	0.1783(1)	2.49(5)
Cl(3)	0.76109(9)	0.4722(1)	0.2256(1)	2.60(5)
Cl(4)	0.62996(9)	0.5654(1)	0.1883(1)	2.70(5)
P(1)	0.68852(8)	0.7244(1)	0.2468(1)	1.82(5)
P(2)	0.78078(8)	0.5231(1)	0.4420(1)	1.69(4)
P(3)	0.80612(8)	0.6665(1)	0.3870(1)	1.51(4)
P(4)	0.64565(8)	0.5183(1)	0.3938(1)	1.83(5)
C(1)	0.6771(3)	0.7403(5)	0.1346(6)	2.4(2)
C(2)	0.7024(7)	0.7819(9)	0.0962(8)	9.3(4)
C(3)	0.6918(6)	0.7931(8)	0.0076(8)	8.3(4)
C(4)	0.6535(5)	0.7672(6)	–0.0389(7)	4.6(3)
C(5)	0.6343(8)	0.717(1)	0.090(1)	16.5(5)
C(6)	0.6233(9)	0.731(1)	0.001(1)	19.2(7)
C(7)	0.6386(3)	0.7778(5)	0.2793(6)	2.4(2)
C(8)	0.6431(4)	0.8457(5)	0.2780(6)	2.7(2)
C(9)	0.6044(4)	0.8866(6)	0.3016(7)	3.9(3)
C(10)	0.5603(4)	0.8565(6)	0.3251(7)	4.2(3)
C(11)	0.5562(4)	0.7886(7)	0.3270(8)	4.9(3)
C(12)	0.5949(4)	0.7480(6)	0.3027(7)	3.8(3)
C(13)	0.7513(3)	0.7655(5)	0.2831(5)	2.0(2)
C(14)	0.7773(3)	0.7494(4)	0.3764(5)	1.6(2)
C(15)	0.8738(3)	0.6803(4)	0.3739(5)	1.9(2)
C(16)	0.9042(3)	0.7249(5)	0.4274(6)	2.5(2)
C(17)	0.9571(4)	0.7297(5)	0.4265(6)	2.9(2)
C(18)	0.9794(3)	0.6890(5)	0.3713(7)	3.2(2)
C(19)	0.9499(4)	0.6445(6)	0.3195(7)	3.6(2)
C(20)	0.8960(3)	0.6397(5)	0.3198(6)	2.7(2)
C(21)	0.8180(3)	0.6461(5)	0.5019(5)	2.0(2)
C(22)	0.7854(3)	0.5875(5)	0.5234(5)	1.9(2)
C(23)	0.8456(3)	0.4859(4)	0.4648(6)	2.1(2)
C(24)	0.8673(4)	0.4687(6)	0.5465(7)	4.0(3)
C(25)	0.9168(5)	0.4431(6)	0.5628(7)	4.3(3)
C(26)	0.9463(4)	0.4350(7)	0.5001(8)	4.6(3)
C(27)	0.9234(4)	0.4515(7)	0.4184(8)	5.2(3)
C(28)	0.8730(3)	0.4763(5)	0.3990(6)	3.0(2)
C(29)	0.7385(3)	0.4608(5)	0.4774(6)	2.2(2)
C(30)	0.6858(3)	0.4898(5)	0.4921(5)	2.2(2)
C(31)	0.6206(3)	0.4432(5)	0.3418(5)	2.1(2)
C(32)	0.6467(3)	0.4135(5)	0.2829(6)	2.7(2)
C(33)	0.6290(4)	0.3545(6)	0.2448(7)	3.7(2)
C(34)	0.5849(4)	0.3233(5)	0.2666(7)	3.2(2)
C(35)	0.5580(4)	0.3551(6)	0.3224(7)	3.9(2)
C(36)	0.5754(4)	0.4133(6)	0.3608(6)	3.5(2)
C(37)	0.5884(3)	0.5538(5)	0.4272(5)	2.3(2)
C(38)	0.5831(4)	0.5591(5)	0.5125(6)	2.5(2)
C(39)	0.4993(4)	0.6092(5)	0.4692(6)	3.1(2)
C(40)	0.5375(4)	0.5861(6)	0.5315(6)	3.4(2)
C(41)	0.5046(4)	0.6047(5)	0.3853(6)	3.0(2)
C(42)	0.5491(3)	0.5768(5)	0.3646(6)	2.8(2)

[a] Values for anisotropically refined atoms are given in the form of the equivalent isotropic displacement parameter defined as $^1/_3[a^2a^{*2}B_{11} + b^2b^{*2}B_{22} + c^2c^{*2}B_{33} + 2ab(\cos\gamma)a^*b^*B_{12} + 2ac(\cos\beta)a^*c^*B_{13} + 2bc(\cos\alpha)b^*c^*B_{23}]$.

trimethylbromosilane were purchased from Aldrich Inc. and used as received. $Mo_2(O_2CCF_3)_4$[9] and $K_4Mo_2Cl_8$[10] were prepared according to the published procedures. The UV/vis data were collected on a Cary 17-D spectrophotometer. The variable-temperature $^{31}P\{^1H\}$ NMR spectra were recorded at 80.96 MHz on a Varian XL-200 spectrometer with 10° intervals in a CD_2Cl_2/CH_2Cl_2 (1:3) solvent mixture and with a preaquisition delay of 10 min. A total of 300 transients were recorded at each temperature, and the $^{31}P\{^1H\}$ NMR chemical shift values were referenced externally and are reported relative to 85% H_3PO_4. Analyses were done by Galbraith Laboratories, Inc.

Preparation of *rac*-Mo_2Cl_4(tetraphos-1)·CH_2Cl_2 (1) and *meso*-Mo_2Cl_4(tetraphos-1) (2).

Method 1. $K_4Mo_2Cl_8$ (0.10 g, 0.16 mmol) and tetraphos-1 (0.21 g, 0.32 mmol) were placed in a three-neck flask equipped with a reflux condenser. Methanol (15 mL) was then added. This mixture was refluxed for 15 h to yield a brown solution and a brown solid. The solid was filtered off, washed with methanol and ether, and then vacuum dried overnight. Yield: 64–85% of a mixture of the meso and racemic diastereomers.

Method 2. In a 50-mL flask, $Mo_2(O_2CCF_3)_4$ (0.30 g, 0.47 mmol) and tetraphos-1 (0.32 g, 0.48 mmol) were dissolved in 30 mL of THF, and then Me_3SiCl (0.4 mL, 3.2 mmol) was added. The reaction mixture first turned to green and soon a brown precipitate began to form, while the solution also changed to brown. After 21 h, solvent THF was evaporated and the brown residue was washed with hexane and filtered. The brown solid thus obtained was dried under reduced pressure. Yield: 70–85% of the mixture.

Crystals of both the meso and racemic diastereomers **1** and **2** can be obtained by slow diffusion of hexane into CH_2Cl_2 solution of the products from either of the reactions, and they were separated under a microscope because of the different colors and shapes of the crystals (brown needles for **1** and orange-red rhomboids for **2**). Anal. Calcd for $Mo_2Cl_4P_4C_{42}H_{42}$: C, 50.07; H, 4.21. Found: C, 48.94; H, 4.41. UV/vis of **1**: 720 nm (370 M^{-1} cm^{-1}), 475 nm (860 M^{-1} cm^{-1}), 405 nm (700 M^{-1} cm^{-1}). UV/vis of **2**: 815 nm (400 M^{-1} cm^{-1}), 475 nm (570 M^{-1} cm^{-1}), 350 nm (3280 M^{-1} cm^{-1}).

Preparation of *rac*-Mo_2Br_4(tetraphos-1)·0.5CH_2Cl_2 (3), *meso*-Mo_2Br_4(tetraphos-1)·CH_2Cl_2 (4), and *meso*-Mo_2Br_4(tetraphos-1)·1.5 THF (5). $Mo_2(O_2CCF_3)_4$ (0.30 g, 0.47 mmol), tetraphos-1 (0.32 g, 0.48 mmol), and excess Me_3SiBr (0.5 mL, 4.6 mmol) were mixed together in THF and stirred at room temperature for 17 h. The brown precipitate thus formed was isolated by filtration, washed with hexane and vacuum dried overnight. Yield: 60–80%.

Crystals of both **3** and **4** were obtained by hexane-induced crystallization from a CH_2Cl_2 solution of this brown product. They were separated under a microscope on the basis of the different shapes and colors of the crystals (brown needles for **3** and brown-red rhomboids for **4**). Red prismatic crystals of **5** were obtained by slow diffusion of hexane into the THF mother liquor. Anal. Calcd for $Mo_2Br_4P_4C_{42}H_{42}$: C, 42.67; H, 3.59. Found: C, 41.09; H, 3.60. UV/vis of **3**: 770 nm (390 M^{-1} cm^{-1}), 450 nm (315 M^{-1} cm^{-1}), 370 nm (1460 M^{-1} cm^{-1}). UV/vis of **5**: 870 nm (300 M^{-1} cm^{-1}), 480 nm (640 M^{-1} cm^{-1}), 382 nm (4645 M^{-1} cm^{-1}).

Table IV. Positional and Thermal Parameters for Non-Hydrogen Atoms of *rac*-Mo_2Br_4(tetraphos-1)·0.5CH_2Cl_2 (**3**)

atom	x	y	z	B_{eq},[a] Å^2
Mo(1)	0.44806(2)	0.34016(3)	0.19887(3)	1.367(9)
Br(1)	0.46388(3)	0.37389(3)	0.01937(4)	2.13(1)
Br(2)	0.41027(3)	0.20987(3)	0.14891(5)	2.24(1)
P(1)	0.36666(8)	0.32984(8)	0.3211(1)	1.73(3)
P(2)	0.40919(8)	0.46884(8)	0.2145(1)	1.76(3)
C(1)	0.3825(3)	0.2651(3)	0.4280(4)	1.9(1)
C(2)	0.3462(4)	0.2742(4)	0.5041(5)	3.1(1)
C(3)	0.3618(4)	0.2292(5)	0.5925(6)	3.8(2)
C(4)	0.4123(4)	0.1756(4)	0.6005(5)	3.4(2)
C(5)	0.4473(4)	0.1651(4)	0.5236(6)	3.2(2)
C(6)	0.4313(3)	0.2104(4)	0.4365(5)	2.5(1)
C(7)	0.2765(3)	0.3080(3)	0.2495(4)	1.8(1)
C(8)	0.2262(4)	0.3609(4)	0.2149(5)	3.0(1)
C(9)	0.1595(4)	0.3431(4)	0.1569(6)	3.5(2)
C(10)	0.1429(4)	0.2699(5)	0.1339(5)	3.8(2)
C(11)	0.1918(3)	0.2161(4)	0.1684(5)	3.0(1)
C(12)	0.2587(3)	0.2341(4)	0.2264(5)	2.6(1)
C(13)	0.3577(3)	0.4181(4)	0.3846(5)	2.3(1)
C(14)	0.3891(4)	0.4832(3)	0.3403(5)	2.5(1)
C(15)	0.4648(3)	0.5487(4)	0.2087(5)	2.6(1)
C(16)	0.3262(3)	0.4899(3)	0.1200(5)	2.1(1)
C(17)	0.2907(3)	0.5542(4)	0.1274(5)	2.9(1)
C(18)	0.2257(4)	0.5680(4)	0.0621(6)	3.6(2)
C(19)	0.1965(4)	0.5170(4)	–0.0130(6)	3.5(2)
C(20)	0.2313(4)	0.4539(4)	–0.0222(5)	3.1(1)
C(21)	0.2960(3)	0.4395(4)	0.0442(5)	2.7(1)
C(22)	0.500	0.043(1)	0.250	30(3)
Cl(1)	0.5495(5)	–0.0027(3)	0.6960(6)	22.4(3)

[a] Values for anisotropically refined atoms are given in the form of the equivalent isotropic displacement parameter defined as $^1/_3[a^2a^{*2}B_{11} + b^2b^{*2}B_{22} + c^2c^{*2}B_{33} + 2ab(\cos\gamma)a^*b^*B_{12} + 2ac(\cos\beta)a^*c^*B_{13} + 2bc(\cos\alpha)b^*c^*B_{23}]$.

(9) Cotton, F. A.; Norman, J. G. *J. Coord. Chem.* **1971**, *1*, 161.
(10) Cotton, F. A.; Brencic, J. V. *Inorg. Chem.* **1970**, *9*, 351.

Table V. Positional and Thermal Parameters for Non-Hydrogen Atoms of *meso*-Mo^4–MoBr$_4$(tetraphos-1)·CH$_2$Cl$_2$ (**4**)

atom	*x*	*y*	*z*	B_{eq},[a] Å^2	atom	*x*	*y*	*z*	B_{eq},[a] Å^2
Mo(1)	0.4322(1)	0.5723(1)	0.32592(9)	2.10(5)	C(35)	0.402(2)	0.832(2)	0.435(1)	7(1)*
Mo(2)	0.4519(1)	0.6002(1)	0.24552(9)	2.06(5)	C(36)	0.363(2)	0.771(2)	0.426(1)	5.0(8)*
Mo(3)	1.0769(2)	0.2812(1)	0.18894(9)	2.33(6)	C(37)	0.305(2)	0.636(1)	0.426(1)	2.5(6)*
Mo(4)	1.0515(1)	0.2461(1)	0.26619(9)	2.26(5)	C(38)	0.220(2)	0.636(2)	0.437(1)	5.7(9)*
Br(1)	0.3008(2)	0.5111(2)	0.3413(1)	3.84(8)	C(39)	0.197(2)	0.620(2)	0.488(1)	6(1)*
Br(2)	0.5752(2)	0.5446(2)	0.2089(1)	3.82(8)	C(40)	0.254(2)	0.606(2)	0.524(1)	5.6(9)*
Br(3)	0.5320(2)	0.7040(2)	0.2376(1)	3.96(8)	C(41)	0.334(2)	0.604(2)	0.515(1)	5.8(9)*
Br(4)	0.5480(2)	0.6165(2)	0.3794(1)	3.47(8)	C(42)	0.361(2)	0.621(1)	0.464(1)	3.8(7)*
Br(5)	1.2062(2)	0.3477(2)	0.1852(1)	3.97(8)	C(43)	1.043(2)	0.440(1)	0.149(1)	3.2(7)*
Br(6)	0.9176(2)	0.2917(2)	0.2951(1)	4.06(8)	C(44)	1.053(2)	0.408(2)	0.100(1)	4.2(7)*
Br(7)	0.9839(2)	0.1375(2)	0.2597(1)	4.45(9)	C(45)	1.084(3)	0.447(2)	0.060(2)	10(1)*
Br(8)	0.9706(2)	0.2354(2)	0.1281(1)	3.74(8)	C(46)	1.099(2)	0.511(2)	0.067(1)	6.2(9)*
P(1)	0.4947(5)	0.4613(4)	0.3185(3)	2.9(2)	C(47)	1.089(2)	0.536(1)	0.113(1)	3.8(7)*
P(2)	0.3735(5)	0.5127(4)	0.2050(3)	2.6(2)	C(48)	1.059(2)	0.504(2)	0.155(1)	5.0(8)*
P(3)	0.3162(5)	0.6487(4)	0.2283(3)	2.9(2)	C(49)	0.896(2)	0.402(1)	0.191(1)	2.9(6)*
P(4)	0.3465(5)	0.6626(4)	0.3651(3)	2.5(2)	C(50)	0.841(2)	0.352(2)	0.183(1)	5.0(8)*
P(5)	1.0051(5)	0.3879(4)	0.1997(3)	2.7(2)	C(51)	0.758(2)	0.368(1)	0.175(1)	3.7(7)*
P(6)	1.1174(5)	0.3344(4)	0.3157(3)	3.2(2)	C(52)	0.728(2)	0.430(1)	0.178(1)	3.3(7)*
P(7)	1.1885(5)	0.1999(4)	0.2881(3)	2.8(2)	C(53)	0.784(2)	0.478(2)	0.188(1)	4.4(8)*
P(8)	1.1778(5)	0.2018(4)	0.1496(3)	2.8(2)	C(54)	0.867(2)	0.462(1)	0.195(1)	3.5(7)*
C(1)	0.461(2)	0.418(1)	0.374(1)	3.3(7)*	C(55)	1.025(1)	0.429(1)	0.2620(9)	2.0(5)*
C(2)	0.463(2)	0.448(1)	0.423(1)	3.5(7)*	C(56)	1.115(2)	0.415(1)	0.287(1)	3.8(7)*
C(3)	0.433(2)	0.417(2)	0.470(1)	5.5(9)*	C(57)	1.077(2)	0.347(2)	0.381(1)	4.5(8)*
C(4)	0.412(2)	0.359(2)	0.466(1)	7(1)*	C(58)	1.106(2)	0.400(2)	0.406(1)	8(1)*
C(5)	0.412(2)	0.325(2)	0.419(1)	7(1)*	C(59)	1.077(3)	0.408(2)	0.461(2)	8(1)*
C(6)	0.437(2)	0.353(2)	0.372(1)	4.6(8)*	C(60)	1.033(2)	0.363(2)	0.483(1)	7(1)*
C(7)	0.603(2)	0.443(1)	0.321(1)	2.7(6)*	C(61)	1.013(2)	0.307(2)	0.460(1)	6(1)*
C(8)	0.660(2)	0.492(1)	0.322(1)	2.9(6)*	C(62)	1.039(2)	0.302(2)	0.407(1)	5.8(9)*
C(9)	0.747(2)	0.478(2)	0.323(1)	4.4(8)*	C(63)	1.227(2)	0.316(2)	0.333(1)	4.2(8)*
C(10)	0.772(2)	0.414(2)	0.322(1)	4.8(8)*	C(64)	1.260(2)	0.263(1)	0.299(1)	2.8(6)*
C(11)	0.714(2)	0.372(2)	0.319(1)	4.5(8)*	C(65)	1.196(2)	0.153(2)	0.345(1)	4.5(8)*
C(12)	0.624(2)	0.377(2)	0.320(1)	5.1(8)*	C(66)	1.270(2)	0.131(2)	0.364(1)	4.8(8)*
C(13)	0.462(2)	0.415(2)	0.260(1)	5.1(8)*	C(67)	1.277(2)	0.091(2)	0.408(1)	4.7(8)*
C(14)	0.387(2)	0.435(2)	0.232(1)	4.5(8)*	C(68)	1.207(2)	0.069(2)	0.431(1)	7(1)*
C(15)	0.389(2)	0.502(1)	0.136(1)	3.2(7)*	C(69)	1.131(2)	0.089(2)	0.412(1)	6(1)*
C(16)	0.347(2)	0.452(1)	0.109(1)	3.9(7)*	C(70)	1.122(2)	0.127(1)	0.369(1)	3.6(7)*
C(17)	0.354(2)	0.452(2)	0.054(1)	4.9(8)*	C(71)	1.240(2)	0.147(1)	0.242(1)	2.7(6)*
C(18)	0.393(3)	0.499(2)	0.027(1)	8(1)*	C(72)	1.266(2)	0.183(1)	0.192(1)	2.6(6)*
C(19)	0.434(2)	0.544(2)	0.055(1)	5.4(9)*	C(73)	1.149(2)	0.127(1)	0.124(1)	2.5(6)*
C(20)	0.432(2)	0.549(2)	0.110(1)	4.8(8)*	C(74)	1.080(2)	0.097(1)	0.139(1)	3.6(7)*
C(21)	0.260(2)	0.528(1)	0.204(1)	3.5(7)*	C(75)	1.053(2)	0.038(1)	0.122(1)	3.7(7)*
C(22)	0.240(2)	0.587(1)	0.229(1)	2.8(6)*	C(76)	1.105(2)	0.007(2)	0.084(1)	4.7(8)*
C(23)	0.305(2)	0.688(1)	0.165(1)	2.5(6)*	C(77)	1.175(2)	0.036(2)	0.069(1)	7(1)*
C(24)	0.373(2)	0.701(2)	0.138(1)	4.2(7)*	C(78)	1.199(2)	0.094(2)	0.088(1)	4.1(7)*
C(25)	0.366(2)	0.734(2)	0.089(1)	5.1(8)*	C(79)	1.228(2)	0.236(1)	0.093(1)	3.0(6)*
C(26)	0.284(2)	0.739(2)	0.070(1)	5.4(9)*	C(80)	1.173(2)	0.253(1)	0.052(1)	3.2(6)*
C(27)	0.216(2)	0.724(2)	0.096(1)	5.3(8)*	C(81)	1.201(2)	0.277(2)	0.006(1)	5.9(9)*
C(28)	0.228(2)	0.695(1)	0.143(1)	3.4(7)*	C(82)	1.286(2)	0.288(2)	0.004(1)	5.1(8)*
C(29)	0.275(2)	0.712(1)	0.272(1)	3.4(7)*	C(83)	1.338(2)	0.276(2)	0.045(1)	5.4(9)*
C(30)	0.253(2)	0.686(1)	0.328(1)	2.5(6)*	C(84)	1.311(2)	0.249(2)	0.091(1)	4.4(8)*
C(31)	0.390(2)	0.739(1)	0.381(1)	3.5(7)*	C(85)	0.140(4)	0.657(3)	0.956(2)	15(2)*
C(32)	0.454(2)	0.765(2)	0.349(1)	4.5(8)*	Cl(1)	0.060(1)	0.660(1)	1.0029(8)	20.0(8)*
C(33)	0.487(2)	0.826(2)	0.365(1)	5.2(8)*	Cl(2)	0.212(2)	0.604(1)	0.975(1)	25(1)*
C(34)	0.454(2)	0.860(2)	0.405(1)	5.8(9)*					

[a] Values for anisotropically refined atoms are given in the form of the equivalent isotropic displacement parameter defined as $^1/_3[a^2a^{*2}B_{11} + b^2b^{*2}B_{22} + c^2c^{*2}B_{33} + 2ab(\cos\gamma)a^*b^*B_{12} + 2ac(\cos\beta)a^*c^*B_{13} + 2bc(\cos\alpha)b^*c^*B_{23}]$. Starred values denote atoms that were refined isotropically.

X-ray Crystallography

The structures of compounds **1**–**5** were determined by a general procedure that has been fully described elsewhere.[11] Data reduction was carried out by standard methods with the use of well-established computational procedures.[12] The computations were done with Enraf-Nonius SDP and SHELX-76 software on a VAX computer. The structure factors were obtained after a Lorentz and polarization correction. Empirical absorption corrections based on azimuthal (ψ) scans of reflections of Eulerian angle χ near 90° were applied to all the data.[13] Pertinent crystallographic information on all structures is given in Table I. Tables II–VI list the positional and thermal parameters for complexes **1**–**5**, respectively. Tables VII–XI list the selected bond distances and angles for each of the structures. Tables of anisotropic thermal parameters, complete bond lengths and angles, and complete torsional angles along the Mo^4–Mo bond are available as supplementary material.

Compound 1. A brown needle crystal with dimensions of 0.48 × 0.35 × 0.18 mm was sealed inside a Lindemann capillary with epoxy cement. Crystal quality was verified by means of a rotation photograph. The unit cell constants were determined from the geometrical parameters of 25 well-centered reflections with 2θ values in the range from 18 to 32°. The unit cell constants and axial photographs were consistent with a monoclinic lattice, and the space group was subsequently determined to be $C2/c$. The diffraction data were collected on an Enraf-Nonius CAD-4 diffractometer at 20 °C which was equipped with graphite-monochromated Mo Kα ($\lambda\alpha$ = 0.710 73 Å) radiation. The intensities of all reflections with 2θ values in the range 4–50° were measured by the ω–2θ scan technique. The positions of the two molybdenum atoms were

(11) (a) Bino, A.; Cotton, F. A.; Fanwick, P. E. *Inorg. Chem.* **1979**, *18*, 3558. (b) Cotton, F. A.; Frenz, B. A.; Deganello, G.; Shaver, A. *J. Organomet. Chem.* **1979**, *50*, 227.

(12) Crystallographic computing was done on a local area VAX cluster employing the VAX/VMS V4.6 computer.

(13) North, A. C. T.; Phillips, D. C.; Mathews, F. S. *Acta Crystallogr., Sect. A* **1968**, *24*, 351.

Table VI. Positional and Thermal Parameters for Non-Hydrogen Atoms of *meso*-Mo$_2^4$MoBr$_4$(tetraphos-1)·1.5THF (**5**)

atom	x	y	z	B_{eq},[a] Å^2
Mo(1)	0.22549(5)	0.12286(6)	0.03241(6)	2.48(3)
Mo(2)	0.33214(5)	0.16850(6)	0.11107(6)	2.38(3)
Br(1)	0.21701(7)	0.04904(7)	-0.10822(8)	3.58(4)
Br(2)	0.38685(7)	0.10785(7)	0.26595(8)	3.65(4)
Br(3)	0.31964(7)	0.29385(7)	0.18369(8)	3.81(4)
Br(4)	0.14072(7)	0.16480(8)	0.10782(8)	3.73(4)
P(1)	0.2468(2)	-0.0078(2)	0.1050(2)	2.91(9)
P(2)	0.4009(2)	0.0728(2)	0.0599(2)	2.80(8)
P(3)	0.3593(2)	0.2430(2)	-0.0049(2)	2.86(8)
P(4)	0.1670(2)	0.2201(2)	-0.0922(2)	2.91(8)
C(1)	0.2410(6)	0.5327(7)	0.7137(8)	3.6(3)
C(2)	0.2302(7)	0.0225(8)	0.2697(9)	4.2(4)
C(3)	0.2272(8)	0.0027(9)	0.353(1)	5.2(4)
C(4)	0.2335(8)	0.926(1)	0.379(1)	6.7(5)
C(5)	0.2428(8)	-0.130(1)	0.320(1)	6.1(4)
C(6)	0.2450(7)	-0.1094(8)	0.2343(9)	4.8(4)
C(7)	0.1793(7)	-0.0716(7)	0.0303(8)	3.8(3)
C(8)	0.1068(8)	-0.0529(9)	0.017(1)	6.2(4)
C(9)	0.050(1)	0.596(1)	0.462(1)	7.9(5)
C(10)	0.064(1)	0.657(1)	0.415(1)	8.6(5)
C(11)	0.135(1)	-0.175(1)	-0.071(1)	7.3(5)
C(12)	0.1931(9)	-0.1308(8)	-0.0131(9)	5.7(4)
C(13)	0.3353(7)	-0.0499(7)	0.1179(9)	3.7(3)
C(14)	0.3679(7)	-0.0264(6)	0.0474(8)	3.2(3)
C(15)	0.4978(6)	0.0617(7)	0.1300(8)	3.1(3)
C(16)	0.5500(7)	0.1004(8)	0.1081(9)	4.1(4)
C(17)	0.3764(8)	0.5892(9)	0.339(1)	5.2(4)
C(18)	0.6431(8)	0.0376(9)	0.2320(9)	5.3(4)
C(19)	0.5893(8)	-0.0033(9)	0.2513(9)	4.8(4)
C(20)	0.5173(7)	0.0113(8)	0.2019(8)	4.2(4)
C(21)	0.3994(7)	0.0983(7)	-0.0518(7)	3.2(3)
C(22)	0.4049(6)	0.1857(7)	-0.0647(8)	3.4(3)
C(23)	0.4265(6)	0.3155(7)	0.0464(8)	3.1(3)
C(24)	0.4149(8)	0.3900(8)	0.025(1)	5.2(4)
C(25)	0.469(1)	0.0569(9)	0.563(1)	6.2(5)
C(26)	0.536(1)	0.421(1)	0.125(1)	7.1(5)
C(27)	0.5467(9)	0.345(1)	0.148(1)	6.5(5)
C(28)	0.4918(8)	0.2934(8)	0.111(1)	5.6(4)
C(29)	0.2906(7)	0.2954(8)	-0.0942(8)	4.1(3)
C(30)	0.2259(6)	0.2445(8)	-0.1538(7)	3.6(3)
C(31)	0.0866(7)	0.1803(6)	-0.1776(8)	3.4(3)
C(32)	0.0302(8)	0.1605(8)	-0.152(1)	4.9(4)
C(33)	-0.0321(8)	0.1305(9)	-0.214(1)	6.0(4)
C(34)	0.0396(9)	0.8766(9)	0.304(1)	6.1(4)
C(35)	0.0177(8)	0.1447(9)	-0.330(1)	5.7(4)
C(36)	0.0814(8)	0.1744(8)	-0.2681(8)	4.8(4)
C(37)	0.1320(6)	0.3117(7)	-0.0751(8)	3.3(3)
C(38)	0.0883(8)	0.1479(8)	0.350(1)	4.9(4)
C(39)	0.081(1)	0.0476(9)	0.447(1)	6.7(5)
C(40)	0.1268(9)	0.4120(8)	0.025(1)	5.4(4)
C(41)	0.0637(9)	0.4231(9)	-0.139(1)	6.1(5)
C(42)	0.1510(7)	0.3415(8)	0.011(1)	4.7(4)
O(1)	0.4163(9)	0.7106(8)	0.556(1)	10.7(5)
C(43)	0.455(1)	0.732(1)	0.648(1)	10.6(6)
C(44)	0.415(1)	0.796(1)	0.668(2)	12.6(6)
C(45)	0.388(3)	0.831(2)	0.580(2)	24.6(7)
C(46)	0.366(2)	0.771(1)	0.510(2)	13.6(7)
O(2)	0.164(2)	0.880(2)	0.717(2)	13.2(6)*
C(47)	0.162(2)	0.912(2)	0.631(3)	13.2(6)*
C(48)	0.117(3)	0.855(3)	0.559(2)	13.2(6)*
C(49)	0.113(2)	0.783(2)	0.614(3)	13.2(6)*
C(50)	0.173(2)	0.800(2)	0.709(2)	13.2(6)*

[a] Values for anisotropically refined atoms are given in the form of the equivalent isotropic displacement parameter defined as $^1/_3[a^2a^{*2}B_{11} + b^2b^{*2}B_{22} + c^2c^{*2}B_{33} + 2ab(\cos\gamma)a^*b^*B_{12} + 2ac(\cos\beta)a^*c^*B_{13} + 2bc(\cos\alpha)b^*c^*B_{23}]$. Starred values denote atoms that were refined isotropically.

determined from a Patterson map. The positions of the remaining non-hydrogen atoms were located and refined by alternating difference Fourier maps and least-squares cycles. Anisotropic thermal parameters were used for all the atoms.

Compound 2. An orange-red rhomboidal crystal with dimensions of 0.25 × 0.21 × 0.15 mm was mounted on the top of a quartz fiber with epoxy resin and kept at -60 °C during the data collection. Systematic absences narrowed the choice of space groups to $C2/c$ and Cc. The centrosymmetric space group, $C2/c$, was selected for the initial refinement, and this choice proved satisfactory. Diffraction data were collected, via an ω-2θ method, on an Enraf-Nonius CAD-4 diffractometer using monochromated Mo Kα radiation. There was no observable decay during the data collection. Two Mo atoms and their coordinated atoms were found by Patterson methods and the remaining non-hydrogen atoms by a combination of Fourier syntheses and least-squares refinements. All the non-hydrogen atoms were refined anisotropically.

Compound 3. A brown needle crystal of dimensions 0.55 × 0.17 × 0.13 mm was coated with epoxy cement and mounted on the top of a

Table VII. Selected Bond Lengths (Å) and Angles (deg) for *rac*-Mo$_2^4$MoCl$_4$(tetraphos-1)·CH$_2$Cl$_2$ (**1**)[a]

Mo-Mo′	2.1549(4)	P(1)-C(13)	1.846(5)
Mo-Cl(1)	2.400(1)	P(2)-C(14)	1.842(5)
Mo-Cl(2)	2.430(1)	P(2)-C(15)	1.847(6)
Mo-P(1)	2.542(1)	P(2)-C(16)	1.821(4)
Mo-P(2)	2.509(1)	C(13)-C(15)	1.522(8)
P(1)-C(1)	1.827(4)	C(14)′-C(14)	1.552(7)
P(1)-C(7)	1.824(5)		
Mo′-Mo-Cl(1)	108.11(3)	C(1)-P(1)-C(7)	102.8(2)
Mo′-Mo-Cl(2)	107.53(3)	C(1)-P(1)-C(13)	105.0(2)
Mo′-Mo-P(1)	101.82(3)	C(7)-P(1)-C(13)	102.9(2)
Mo′-Mo-P(2)	101.22(3)	Mo-P(2)-C(14)	124.5(2)
Cl(1)-Mo-Cl(2)	94.16(4)	Mo-P(2)-C(15)	109.8(2)
Cl(1)-Mo-P(1)	85.19(4)	Mo-P(2)-C(16)	111.4(2)
Cl(1)-Mo-P(2)	148.11(4)	C(14)-P(2)-C(15)	100.8(3)
Cl(2)-Mo-P(1)	149.24(4)	C(14)-P(2)-C(16)	103.6(2)
Cl(2)-Mo-P(2)	88.64(4)	C(15)-P(2)-C(16)	104.8(3)
P(1)-Mo-P(2)	76.67(4)	P(1)-C(13)-C(15)	114.6(4)
Mo-P(1)-C(1)	109.1(2)	P(2)-C(14)-C(14)′	112.7(4)
Mo-P(1)-C(7)	123.3(2)	P(2)-C(15)-C(13)	115.9(4)
Mo-P(1)-C(13)	112.1(2)		

[a] Numbers in parenthesis are estimated standard deviations in the least significant digit.

Table VIII. Selected Bond Lengths (Å) and Angles (deg) for *meso*-Mo$_2^4$MoCl$_4$(tetraphos-1) (**2**)[a]

Mo(1)-Mo(2)	2.186(1)	P(2)-C(22)	1.836(9)
Mo(1)-Cl(1)	2.412(2)	P(2)-C(23)	1.836(9)
Mo(1)-Cl(4)	2.356(2)	P(2)-C(29)	1.83(1)
Mo(1)-P(1)	2.571(3)	P(3)-C(14)	1.840(9)
Mo(1)-P(4)	2.562(3)	P(3)-C(15)	1.841(9)
Mo(2)-Cl(2)	2.404(2)	P(3)-C(21)	1.862(8)
Mo(2)-Cl(3)	2.426(3)	P(4)-C(30)	1.831(8)
Mo(2)-P(2)	2.502(2)	P(4)-C(31)	1.807(9)
Mo(2)-P(3)	2.476(2)	P(4)-C(37)	1.82(1)
P(1)-C(1)	1.802(9)	C(13)-C(14)	1.57(1)
P(1)-C(7)	1.84(1)	C(21)-C(22)	1.54(1)
P(1)-C(13)	1.845(9)	C(29)-C(30)	1.55(1)
Mo(2)-Mo(1)-Cl(4)	104.18(7)	C(7)-P(1)-C(13)	106.4(4)
Mo(2)-Mo(1)-P(1)	96.94(6)	Mo(2)-P(2)-C(22)	108.6(3)
Mo(2)-Mo(1)-P(4)	105.71(6)	Mo(2)-P(2)-C(23)	113.4(3)
Cl(1)-Mo(1)-Cl(4)	142.57(8)	Mo(2)-P(2)-C(29)	122.8(3)
Cl(1)-Mo(1)-P(1)	83.23(8)	C(22)-P(2)-C(23)	101.9(4)
Cl(1)-Mo(1)-P(4)	81.17(8)	C(22)-P(2)-C(29)	103.8(4)
Cl(4)-Mo(1)-P(1)	94.63(8)	C(23)-P(2)-C(29)	104.0(4)
Cl(4)-Mo(1)-P(4)	87.00(8)	Mo(2)-P(3)-C(14)	118.3(3)
P(1)-Mo(1)-P(4)	156.17(8)	Mo(2)-P(3)-C(15)	114.9(3)
Mo(1)-Mo(2)-Cl(2)	107.35(6)	Mo(2)-P(3)-C(21)	112.3(3)
Mo(1)-Mo(2)-Cl(3)	112.35(6)	C(14)-P(3)-C(15)	103.8(4)
Mo(1)-Mo(2)-P(2)	96.16(6)	C(14)-P(3)-C(21)	106.9(4)
Mo(1)-Mo(2)-P(3)	95.57(6)	C(15)-P(3)-C(21)	98.5(4)
Cl(2)-Mo(2)-Cl(3)	89.01(8)	Mo(1)-P(4)-C(30)	117.8(3)
Cl(2)-Mo(2)-P(2)	153.69(8)	Mo(1)-P(4)-C(31)	120.1(3)
Cl(2)-Mo(2)-P(3)	87.56(8)	Mo(1)-P(4)-C(37)	106.0(3)
Cl(3)-Mo(2)-P(2)	92.91(8)	C(30)-P(4)-C(31)	103.8(4)
Cl(3)-Mo(2)-P(3)	151.58(8)	C(30)-P(4)-C(37)	104.5(4)
P(2)-Mo(2)-P(3)	78.37(7)	C(31)-P(4)-C(37)	102.6(4)
Mo(1)-P(1)-C(1)	123.1(3)	P(1)-C(13)-C(14)	114.9(6)
Mo(1)-P(1)-C(7)	109.3(3)	P(3)-C(14)-C(13)	112.4(6)
Mo(1)-P(1)-C(13)	113.6(3)	P(3)-C(21)-C(22)	113.0(5)
C(1)-P(1)-C(7)	100.1(4)	P(2)-C(22)-C(21)	111.2(6)
P(2)-C(29)-C(30)	112.7(7)	P(4)-C(30)-C(29)	112.4(6)

[a] Numbers in parenthesis are estimated standard deviations in the least significant digit.

Table IX. Selected Bond Lengths (Å) and Angles (deg) for *rac*-Mo^{4}MoBr$_4$(tetraphos-1)·0.5CH_2Cl_2 (**3**)[a]

Mo(1)–Mo(1)′	2.1520(6)	P(1)–C(7)	1.831(5)
Mo(1)–Br(1)	2.5667(8)	P(1)–C(13)	1.855(7)
Mo(1)–Br(2)	2.5388(8)	P(2)–C(14)	1.835(7)
Mo(1)–P(1)	2.552(2)	P(2)–C(15)	1.837(7)
Mo(1)–P(2)	2.501(2)	P(2)–C(16)	1.836(6)
P(1)–C(1)	1.823(6)		
Mo(1)–Mo(1)′–Br(1)	106.31(3)	Mo(1)–P(1)–C(7)	110.8(2)
Mo(1)–Mo(1)′–Br(2)	109.59(3)	Mo(1)–P(1)–C(13)	111.9(2)
Mo(1)–Mo(1)′–P(1)	103.57(4)	Mo(1)–P(2)–C(14)	110.4(2)
Mo(1)–Mo(1)′–P(2)	101.89(4)	Mo(1)–P(2)–C(15)	123.5(2)
Br(1)–Mo(1)–Br(2)	94.30(3)	Mo(1)–P(2)–C(16)	112.1(2)
Br(1)–Mo(1)–P(1)	148.49(4)	C(1)–P(1)–C(7)	102.9(3)
Br(1)–Mo(1)–P(2)	87.72(4)	C(1)–P(1)–C(13)	103.0(3)
Br(2)–Mo(1)–P(1)	84.91(4)	C(7)–P(1)–C(13)	104.0(3)
Br(2)–Mo(1)–P(2)	146.41(4)	C(14)–P(2)–C(15)	100.8(3)
P(1)–Mo(1)–P(2)	76.47(5)	C(14)–P(2)–C(16)	104.3(3)
Mo(1)–P(1)–C(1)	122.4(2)	C(15)–P(2)–C(16)	103.7(3)

[a] Numbers in parenthesis are estimated standard deviations in the least significant digit.

Table X. Selected Bond Lengths (Å) and Angles (deg) for *meso*-Mo^{4}MoBr$_4$(tetraphos-1)·CH_2Cl_2 (**4**)[a]

Mo(1)–Mo(2)	2.195(3)	Mo(3)–Mo(4)	2.183(3)
Mo(1)–Br(1)	2.563(4)	Mo(3)–Br(5)	2.559(4)
Mo(1)–Br(4)	2.514(4)	Mo(3)–Br(8)	2.524(4)
Mo(1)–P(1)	2.592(9)	Mo(3)–P(5)	2.584(8)
Mo(1)–P(4)	2.605(8)	Mo(3)–P(8)	2.592(8)
Mo(2)–Br(2)	2.548(4)	Mo(4)–Br(6)	2.535(4)
Mo(2)–Br(3)	2.588(4)	Mo(4)–Br(7)	2.574(4)
Mo(2)–P(2)	2.488(8)	Mo(4)–P(6)	2.511(9)
Mo(2)–P(3)	2.492(8)	Mo(4)–P(7)	2.513(8)
Mo(2)–Mo(1)–Br(1)	115.3(1)	Mo(4)–Mo(3)–Br(5)	113.6(1)
Mo(2)–Mo(1)–Br(4)	107.1(1)	Mo(4)–Mo(3)–Br(8)	107.2(1)
Mo(2)–Mo(1)–P(1)	96.3(2)	Mo(4)–Mo(3)–P(5)	96.1(2)
Mo(2)–Mo(1)–P(4)	105.1(2)	Mo(4)–Mo(3)–P(8)	105.8(2)
Br(1)–Mo(1)–Br(4)	137.5(1)	Br(5)–Mo(3)–Br(8)	139.1(1)
Br(1)–Mo(1)–P(1)	83.2(2)	Br(5)–Mo(3)–P(5)	84.1(2)
Br(1)–Mo(1)–P(4)	81.5(2)	Br(5)–Mo(3)–P(8)	78.9(2)
Br(4)–Mo(1)–P(1)	95.0(2)	Br(8)–Mo(3)–P(5)	95.5(2)
Br(4)–Mo(1)–P(4)	85.3(2)	Br(8)–Mo(3)–P(8)	86.7(2)
P(1)–Mo(1)–P(4)	157.5(3)	P(5)–Mo(3)–P(8)	156.3(3)
Mo(1)–Mo(2)–Br(2)	111.2(1)	Mo(3)–Mo(4)–Br(6)	108.8(1)
Mo(1)–Mo(2)–Br(3)	113.1(1)	Mo(3)–Mo(4)–Br(7)	109.8(1)
Mo(1)–Mo(2)–P(2)	96.4(2)	Mo(3)–Mo(4)–P(6)	97.0(2)
Mo(1)–Mo(2)–P(3)	97.6(2)	Mo(3)–Mo(4)–P(7)	98.8(2)
Br(2)–Mo(2)–Br(3)	87.7(1)	Br(6)–Mo(4)–Br(7)	89.4(1)
Br(2)–Mo(2)–P(2)	84.4(2)	Br(6)–Mo(4)–P(6)	86.0(2)
Br(2)–Mo(2)–P(3)	147.5(2)	Br(6)–Mo(4)–P(7)	149.8(2)
Br(3)–Mo(2)–P(2)	150.3(2)	Br(7)–Mo(4)–P(6)	152.8(2)
Br(3)–Mo(2)–P(3)	94.9(2)	Br(7)–Mo(4)–P(7)	92.6(2)
P(2)–Mo(2)–P(3)	77.4(3)	P(6)–Mo(4)–P(7)	78.7(3)

[a] Numbers in parenthesis are estimated standard deviations in the least significant digit.

quartz fiber. Diffraction data were collected at −60 °C on an Enraf-Nonius CAD-4 diffractometer using monochromated Mo Kα radiation. The space group $C2/c$ was chosen and confirmed by the successful solution and refinement of the structure. One independent Mo atom of the dinuclear skeleton and its coordinated atoms were determined from a three-dimensional Patterson function. The use of alternating difference Fourier maps and least-squares refinements gave the positions of all the remaining non-hydrogen atoms. The program DIFABS was used to correct for absorption after all non-hydrogen atoms had been located and isotropically refined. All non-hydrogen atoms were then refined anisotropically.

Compound 4. A brown-red rhomboidal crystal with dimensions of 0.62 × 0.35 × 0.20 mm was protected with a 1:1 mixture of mother liquor and deoxygenated mineral oil in a Lindemann capillary. Indexing based on 25 reflections with 2θ ranging from 20 to 26° resulted in a monoclinic cell. The space group was assigned as $P2_1/c$ from the systematic absences in the data. The diffraction data were gathered by a Syntex P3 equivalent diffractometer equipped with Mo Kα radiation. No significant decay was found during the data collection. The direct methods program in

Table XI. Selected Bond Lengths (Å) and Angles (deg) for *meso*-Mo^{4}MoBr$_4$(tetraphos-1)·1.5THF (**5**)[a]

Mo(1)–Mo(2)	2.195(1)	P(1)–C(13)	1.86(1)
Mo(1)–Br(1)	2.558(2)	P(2)–C(14)	1.87(1)
Mo(1)–Br(4)	2.519(2)	P(2)–C(15)	1.86(1)
Mo(1)–P(1)	2.567(3)	P(2)–C(21)	1.83(1)
Mo(1)–P(4)	2.579(3)	P(3)–C(22)	1.85(1)
Mo(2)–Br(2)	2.557(1)	P(3)–C(23)	1.83(1)
Mo(2)–Br(3)	2.571(2)	P(3)–C(29)	1.84(1)
Mo(2)–P(2)	2.504(4)	P(4)–C(30)	1.84(1)
Mo(2)–P(3)	2.495(4)	P(4)–C(31)	1.84(1)
P(1)–C(1)	1.84(1)	P(4)–C(37)	1.83(1)
P(1)–C(7)	1.83(1)		
Mo(2)–Mo(1)–Br(1)	115.86(6)	Br(2)–Mo(2)–P(3)	144.52(8)
Mo(2)–Mo(1)–Br(4)	107.04(6)	Br(3)–Mo(2)–P(2)	153.35(9)
Mo(2)–Mo(1)–P(1)	96.31(8)	Br(3)–Mo(2)–P(3)	87.49(8)
Mo(2)–Mo(1)–P(4)	105.44(7)	P(2)–Mo(2)–P(3)	80.1(1)
Br(1)–Mo(1)–Br(4)	137.04(5)	Mo(1)–P(1)–C(1)	126.1(4)
Br(1)–Mo(1)–P(1)	83.05(8)	Mo(1)–P(1)–C(7)	107.8(4)
Br(1)–Mo(1)–P(4)	78.73(8)	Mo(1)–P(1)–C(13)	114.3(4)
Br(4)–Mo(1)–P(1)	94.7(1)	Mo(2)–P(2)–C(14)	117.8(5)
Br(4)–Mo(1)–P(4)	88.70(9)	Mo(2)–P(2)–C(15)	116.5(4)
P(1)–Mo(1)–P(4)	156.0(1)	Mo(2)–P(2)–C(21)	109.4(4)
Mo(1)–Mo(2)–Br(2)	112.50(6)	Mo(2)–P(3)–C(22)	111.8(4)
Mo(1)–Mo(2)–Br(3)	110.41(6)	Mo(2)–P(3)–C(23)	111.3(4)
Mo(1)–Mo(2)–P(2)	95.19(8)	Mo(2)–P(3)–C(29)	123.2(5)
Mo(1)–Mo(2)–P(3)	101.35(8)	Mo(1)–P(4)–C(30)	112.1(4)
Br(2)–Mo(2)–Br(3)	90.36(5)	Mo(1)–P(4)–C(31)	110.1(4)
Br(2)–Mo(2)–P(2)	86.42(8)	Mo(1)–P(4)–C(37)	124.9(4)

[a] Numbers in parenthesis are estimated standard deviations in the least significant digit.

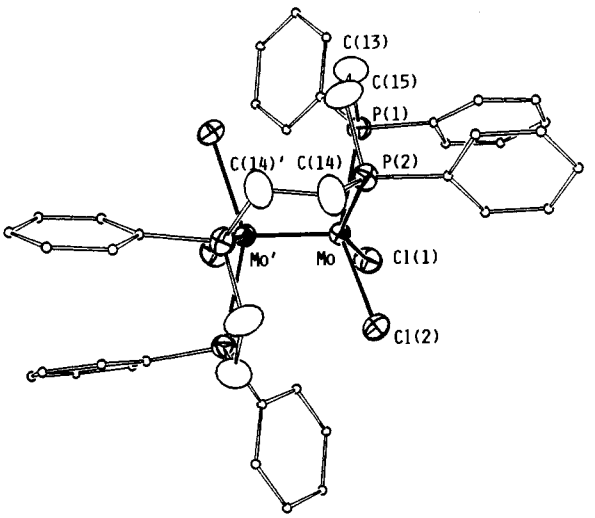

Figure 3. ORTEP drawing of the *R,R*-Mo^{4}MoCl$_4$(tetraphos-1) molecule. Thermal ellipsoids are drawn at the 50% probability level. For clarity, all of the carbon atoms of the phenyl rings are drawn as arbitrarily small circles.

SHELXS-86[14] led to the location of the positions of the molybdenum atoms of two independent molecules A and B. The remaining non-hydrogen atoms were found in a series of alternating difference Fourier maps and least-squares refinements. Anisotropic thermal parameters were used for all the heavy atoms.

Compound 5. A red prismatic crystal with dimensions of 0.60 × 0.20 × 0.20 mm was mounted on the top of a quartz fiber with epoxy cement. Centering, indexing and a least-squares calculation on the 25 reflections with 2θ values 25–30° gave a monoclinic crystal system. The axial photographs confirmed this assignment, and the data were collected on a Syntex P3 Equivalent diffractometer equipped with Mo Kα radiation. The space group $P2_1/c$ is assigned from systematic absences. A Patterson synthesis revealed the locations of the two Mo atoms and their coordinated atoms. By employment of alternate difference Fourier maps and least-squares refinements, the whole molecule and one THF solvent molecule

(14) Sheldrick, G. M. SHELXS-86. Institüt für Anorganische Chemie der Universität, Göttingen, Germany, 1986.

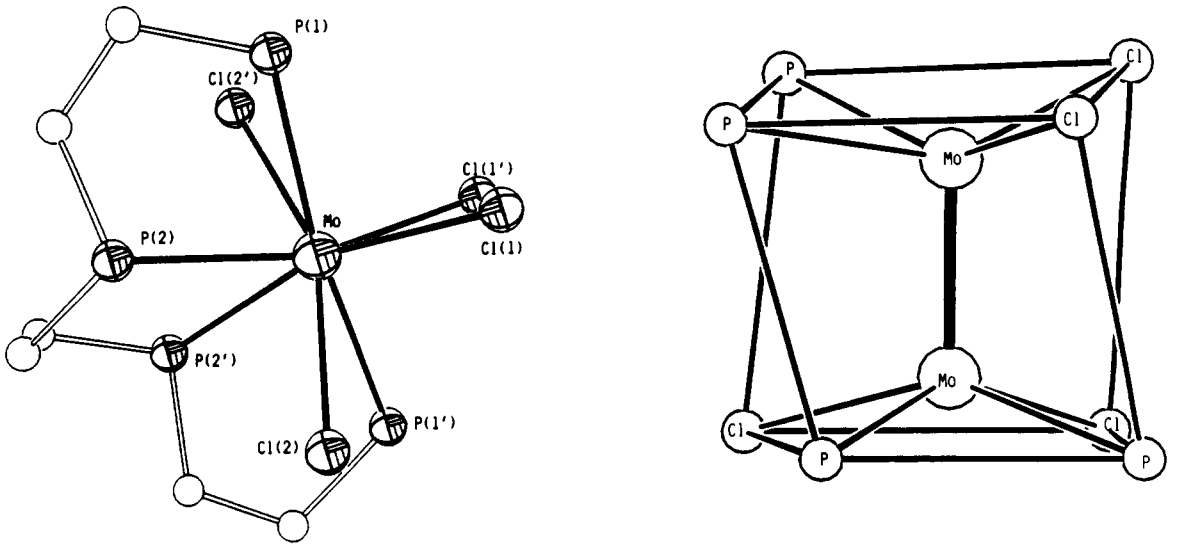

Figure 4. (a) Projection of the inner part of the *R,R*-Mo^4-MoCl$_4$(tetraphos-1) molecule along the Mo–Mo axis. (b) A schematic representation of the inner part of the *R,R*-Mo^4-MoCl$_4$(tetraphos-1) molecule.

Table XII. Comparison of the Structural and Spectroscopic Properties for Complexes **1–5**

complexes	Mo–Mo, Å	χ,[a] deg	av M–P, Å	av M–X, Å	UV–vis, nm	isomer type
1	2.1549(4)	18.5	2.526(1)	2.415(1)	405, 475 720	1,2,6,7/1,2,5,8
2	2.186(1)	30.9(1)	2.528(3)	2.400(3)	350, 475 815	1,2,5,7/1,2,6,8
3	2.1520(6)	19.13(5)	2.527(2)	2.553(4)	370, 450 770	1,2,6,7/1,2,5,8
4 (A)	2.195(3)	30.5(3)	2.544(8)	2.553(4)		1,2,5,7/1,2,6,8
(B)	2.183(3)	30.9(3)	2.550(8)	2.548(4)		
5	2.195(1)	28.6(1)	2.536(4)	2.551(2)	382, 480 870	1,2,5,7/1,2,6,8

[a] The average of four smallest torsional angles.

were obtained and refined to convergence. The THF molecule appeared to be disordered in such a way that unambiguous identification of the oxygen atom was not possible. A single choice was made based on interatomic distances and thermal parameters. However, the difference Fourier map still had five significant peaks which appeared to be another THF solvent molecule. The program SHELX-76 was used to refine the positions of this second solvent molecule. Assignment of the oxygen atom in this THF ring was arbitrary. The C–C and C–O bond lengths were constrained, and only their site occupancies and a common thermal parameter were allowed to refine freely. In the final refinement, the site occupancy for all the five atoms was fixed at 0.500 since the result of the previous free refinement was close to 0.5 with a reasonable thermal parameter. This model was refined to convergence and the final difference electron density map had no significant features other than three small peaks very close to the O(2) atom of the THF molecule.

Results and Discussion

Synthesis and Structure. All *meso*- and *rac*-Mo_2X_4(tetraphos-1) (X = Cl, Br) compounds reported herein can be prepared from the reaction of the quadruply bonded complex, $Mo_2(O_2CCF_3)_4$, with Me_3SiX in the presence of 1 equiv of the tetraphos-1 ligand. *meso* and *rac*-Mo_2Cl_4(tetraphos-1) have also been prepared by a more direct ligand substitution reaction, in which 2 equiv of the ligand were stirred with 1 equiv of $K_4Mo_2Cl_8$ in boiling methanol.

Molecular Structure of *rac*-Mo_2X_4(tetraphos-1) (1 and 3). Crystals of compound **1** conform to the space group $C2/c$ with four molecules per unit cell, and thus a crystallographic C_2 axis passes through the molecule. One molecule is depicted in Figure 3. The 2-fold axis perpendicularly bisects the Mo–Mo bond. Since the two central phosphorus atoms are interrelated by the C_2 axis, they must possess the same chirality, and the molecule shown in Figure 3 has the *R,R* chirality. Since the $C2/c$ space group also contains inversion centers, there are two molecules

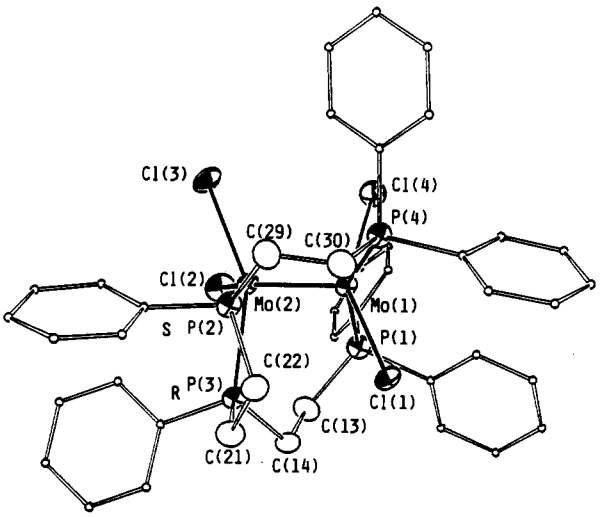

Figure 5. ORTEP drawing of *meso*-Mo^4-MoCl$_4$(tetraphos-1). Thermal ellipsoids are drawn at the 50% probability level. For clarity, all of the carbon atoms of the phenyl rings are drawn as arbitrarily small circles.

with the *R,R* chirality and two with the S,S chirality in each unit cell. Thus we have obtained a racemic *R,R* and *S,S* diastereomer. It can also be seen from Figure 3 that two types of coordination, bridging and chelating, occur in this molecule. Each has been found for the complexes of the type $Mo_2Cl_4(PP)_2$, but separately, namely, the chelating form in α-Mo_2Cl_4(dppe)$_2$ and the bridging form in β-Mo_2Cl_4(dppe)$_2$.[6d] The coordination mode of the tetraphos-1 ligand in **1** is assigned as bischelating/single-bridging.

Figure 4a shows a view of the inner part of an *R,R* molecule of **1** looking down the Mo–Mo bond. This molecule displays a

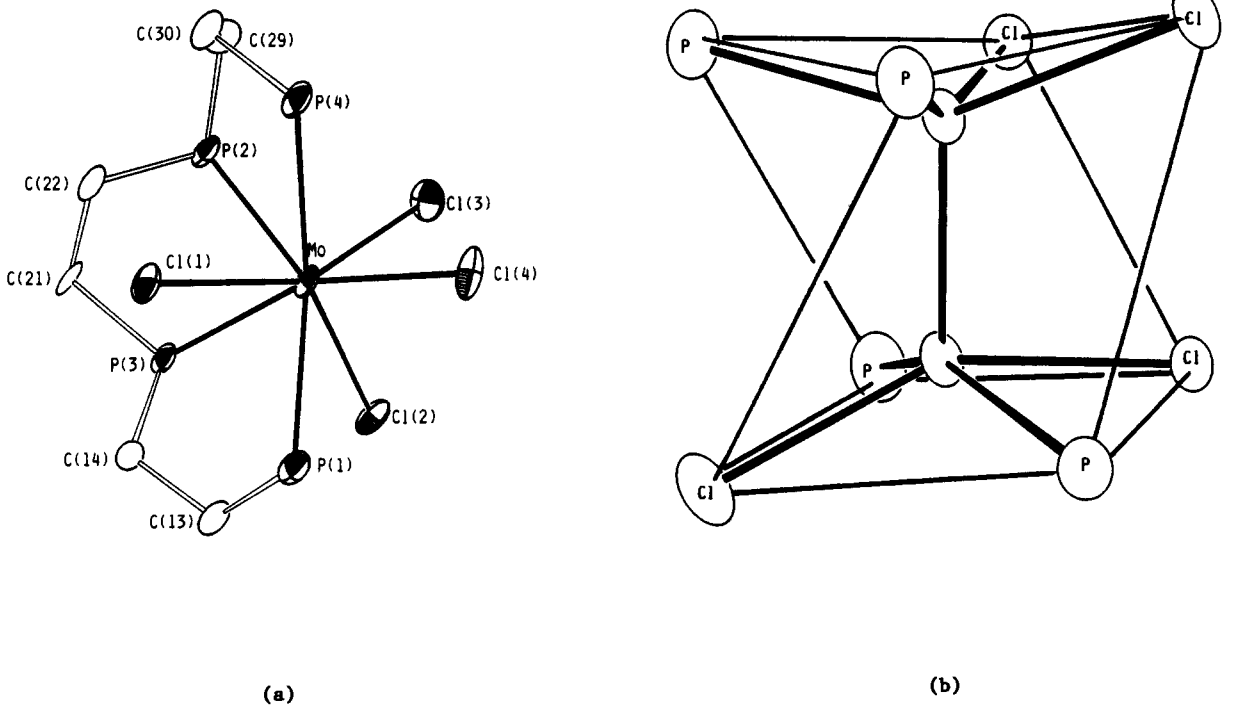

(a) (b)

Figure 6. (a) Projection of the inner part of *meso*-$Mo_2^4MoCl_4$(tetraphos-1) along the Mo–Mo axis. (b) A schematic representation of the inner part of *meso*-$Mo_2^4MoCl_4$(tetraphos-1).

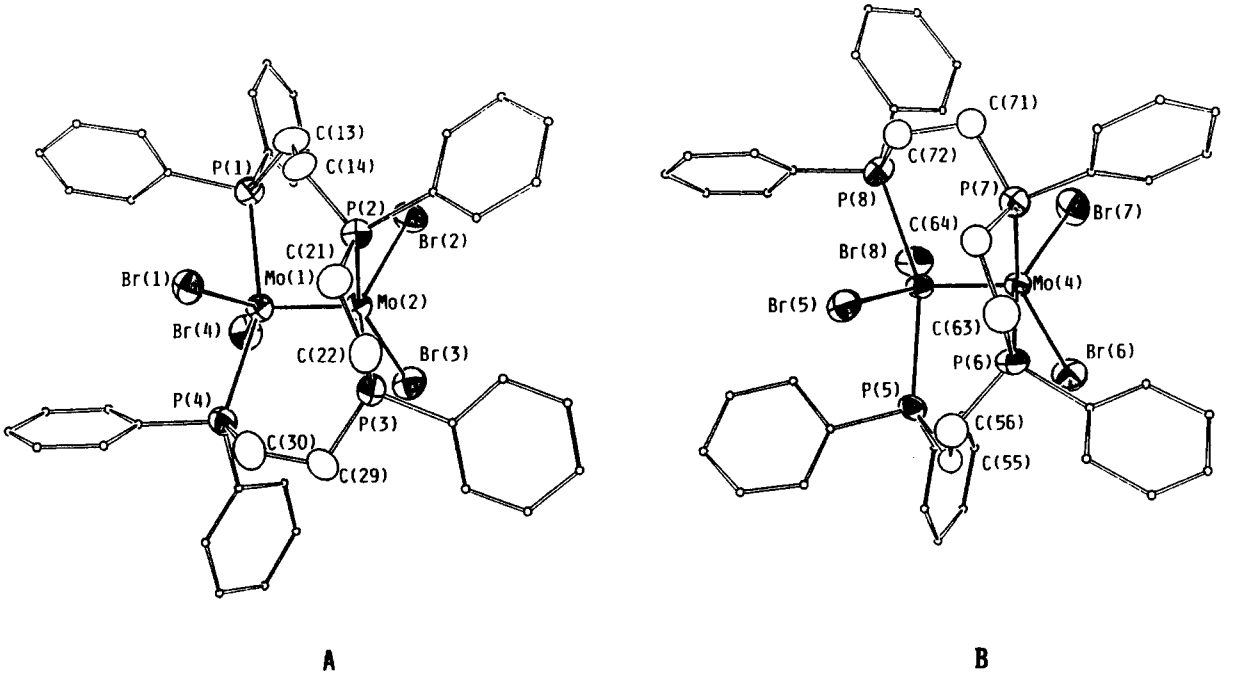

A B

Figure 7. ORTEP drawing of two independent molecules A and B in *meso*-$Mo_2^4MoBr_4$(tetraphos-1)·CH_2Cl_2. Thermal ellipsoids are drawn at the 50% probability level. For clarity, all of the carbon atoms of the phenyl rings are drawn as arbitrarily small circles.

A configuration for the central portion with three different torsional angles. The torsional angle P(2)–Mo–Mo–P(2)′, −31.6°, is similar to the average torsional angle of the complex β-$Mo_2Cl_4(dppe)_2$, which is 30.5°. The other three torsional angles are −18.1, −18.1, and −6.2°, respectively. Thus the average torsional angle for a molecule of **1** is 18.2°. The Mo–Mo distance is 2.1549(4) Å, which is shorter than that of β-$Mo_2Cl_4(dppe)_2$ (2.183(3) Å) but longer than that of α-$Mo_2Cl_4(dppe)_2$ (2.140(2) Å), where the mean torsional angle is 0°. The mean Mo–Cl and Mo–P distances of this compound are 2.415(2) and 2.526(2) Å, respectively. A comparison of bond distances and average torsional angles is presented in Table XII.

Although for notational purposes the $M_2X_4L_4$ are treated as ideal square parallelepipeds, there are significant distortions in many cases. The skeletal view of the inner core of *R,R*-**1**, shown in Figure 4b, makes clear the nature of the distortion. Since the average torsional angle is smaller than 45°, this racemic compound comprises the 1,2,5,8/1,2,6,7 (6) enantiomers, which is a new isomeric structure.

The structure of **3** is crystallographically isomorphous to its chloride analogue **1**. The difference between the average Mo–Cl distance, 2.415(1) Å, and the average Mo–Br distance, 2.553(4) Å, is 0.138 Å, which is about equal to the difference between the standard covalent radii of Br and Cl, 0.15 Å. The torsional angle

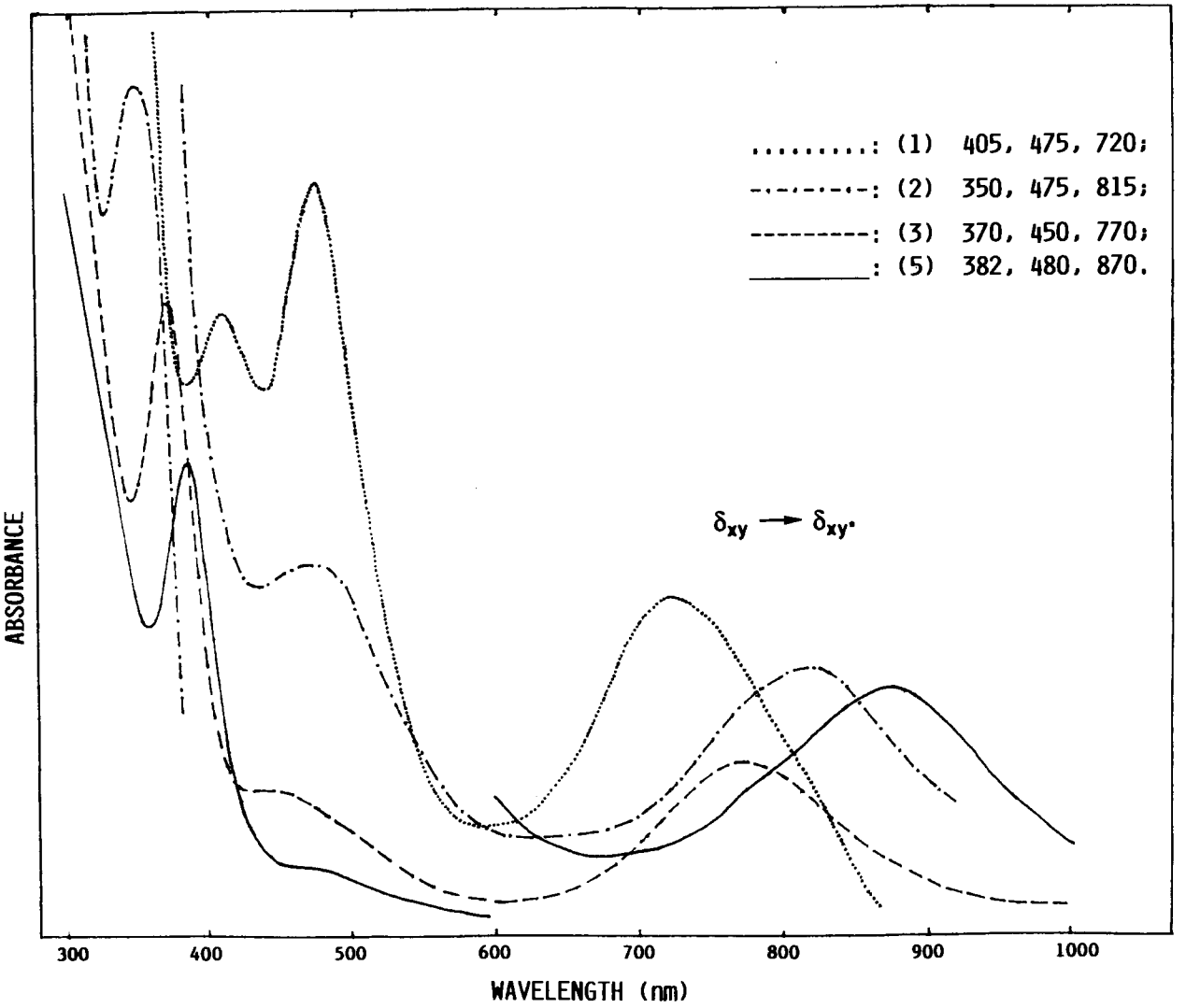

Figure 8. Electronic absorption spectra of **1**, **2**, **3**, and **5** in CH_2Cl_2.

P(2)–Mo–Mo–P(2)′ is −31.2°, and the other three are −18.9, −18.9, and −7.5°. Thus the average torsional angle in **3** is −19.1° for *R,R* molecules with Λ configuration and 19.1° for *S,S* molecules with Δ configuration.

Molecular Structure of *meso*-Mo_2X_4(tetraphos-1) (2, 4, and 5). Compound **2** (X = Cl) also crystallizes in space group $C2/c$, but the molecules reside on general positions, and there are eight molecules per unit cell. Figure 5 displays an ORTEP drawing of the molecule in its entirety. Compared with the previous structure of compound **1**, the obvious difference is that the two central phosphorus atoms now coordinate to the same Mo(2) center and give a meso (*R,S* and *S,R*) diastereomer. The Mo–Mo bond distance is 2.186(1) Å, about 0.031 Å longer than that in **1**. The average Mo–Cl and Mo–P bond distances are 2.400(3) and 2.528(3) Å, which are very close to the values in the racemic diastereomer (Table XII).

The projection along the Mo–Mo axis, as shown in Figure 6a, shows the torsional angles P(4)–Mo(1)–Mo(2)–P(2) as −35.2° and P(1)–Mo(1)–Mo(2)–P(3) as 58.5°. In order to be consistent with the previous discussion in racemic compounds, the four smallest torsional angles are used here. The other three angles have the values of −27.1, −30.4, −30.7°, which give an average of −30.9°. The configuration of the central portion is Λ for the molecule shown in Figure 6a and Δ for its mirror image. As can be seen in Figure 6b, the skeletal drawing of this compound, the structure is highly distorted from cubic, but can be designated as the 1,2,5,7/1,2,6,8 (5) enantiomer. This, too, is another new geometrical isomer. The coordination mode of the tetraphos-1 ligand in **2** is chelating/double-bridging.

The compound *meso*-Mo_2Br_4(tetraphos-1)·CH_2Cl_2 (**4**) has two crystallographically independent but nearly identical molecules, A and B, as shown in Figure 7, in each unit cell. They all reside on general positions in space group $P2_1/c$, and there are eight molecules per unit cell. The Mo–Mo bond distances in A and B molecules are slightly different, 2.195(3) Å for A and 2.183(3) Å for B. The average Mo–P, Mo–Br distances are almost the same for both molecules (Table XII), and the torsional angles of P(4)–Mo(1)–Mo(2)–P(3) and P(8)–Mo(3)–Mo(4)–P(7) are 37.3 and 34.1° for A and B, respectively. All of the possible torsional angles about the Mo–Mo bond have been calculated, and a complete table is available for both Mo(1)–Mo(2) and Mo(3)–Mo(4) in the supplementary material. The average of four smallest torsional angles in each molecule is −30.5° for A and 30.9° for B. There are two Λ and two Δ configurations for the central portions of molecules A and B. Both molecules A and B belong to the 1,2,5,7/1,2,6,8 (5) enantiomer, the same as their chloride analogue.

The compound *meso*-Mo_2Br_4(tetraphos-1)·1.5 THF (**5**) has only one type of independent molecule in each unit cell, with the Mo–Mo bond being 2.195(1) Å. It also crystallizes in $P2_1/c$ with $Z = 4$. Compared with the corresponding torsional angles in A and B in **4**, the torsional angle P(4)–Mo(1)–Mo(2)–P(3) is smaller, −29.11°. The average of the four smallest torsional angles is 28.6°. It also comprises the 1,2,5,7/1,2,6,8 (5) enantiomer.

The average Mo–Mo bond distance in the above three meso compounds is 2.190 Å, about 0.037 Å longer than the average Mo–Mo distance, 2.154 Å, in racemic diastereomers. The corresponding average torsional angle for meso compounds is

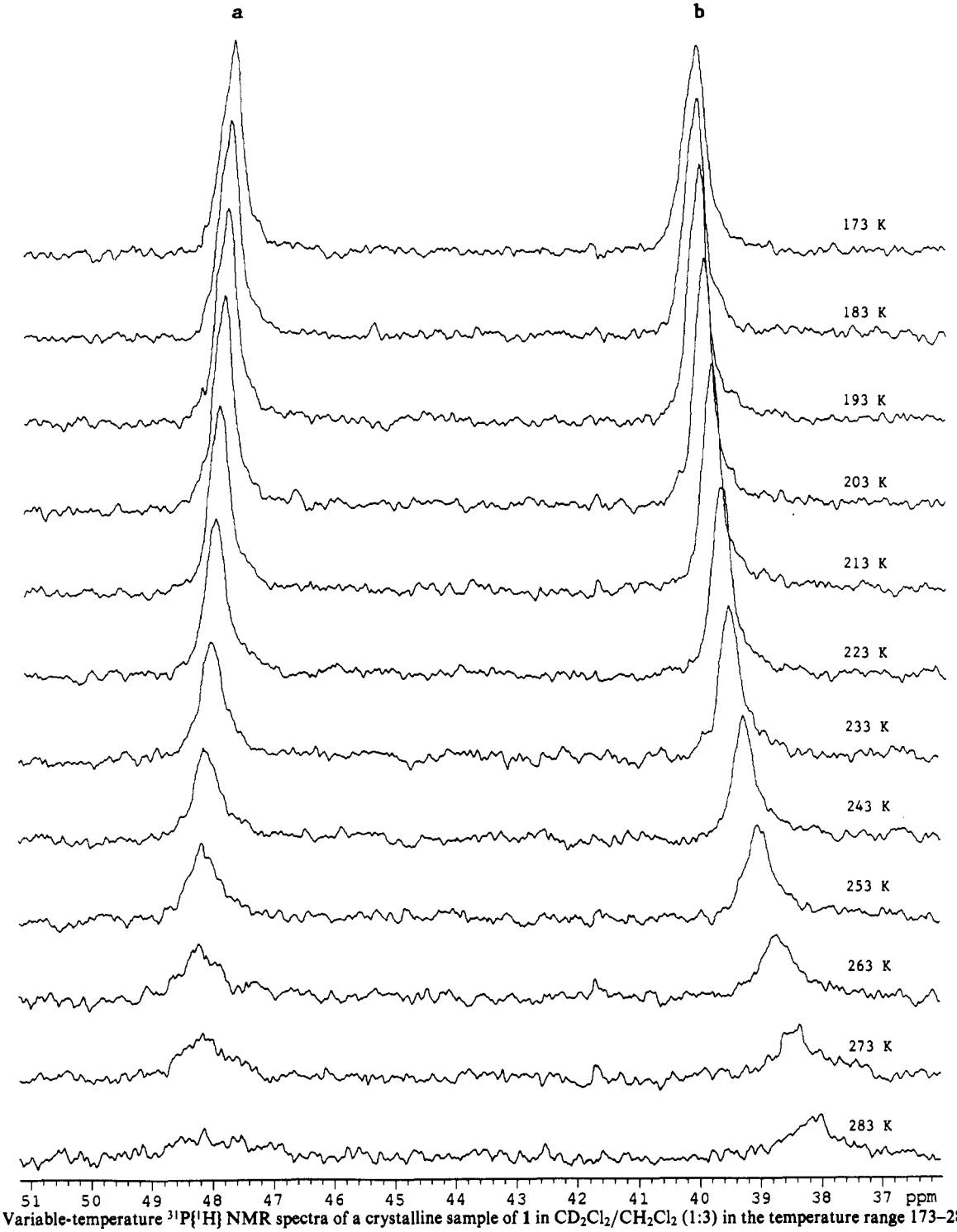

Figure 9. Variable-temperature $^{31}P\{^1H\}$ NMR spectra of a crystalline sample of **1** in CD_2Cl_2/CH_2Cl_2 (1:3) in the temperature range 173–283 K with 10° intervals.

30.0°, and it is 18.8° for racemic ones. These results are consistent with the theoretical expectation that the Mo–Mo quadruple bond distance should vary according to cos 2χ where χ is the average of the four smallest torsional angles about the Mo–Mo bond.

Spectroscopic Properties. UV–Vis Spectroscopy. Figure 8 shows the absorption spectra of the compounds with the tetraphos-1 ligand, using the corresponding crystalline samples separated mechanically. The visible region of each spectrum displays three distinct bands, which are typical for compounds of the type $Mo_2X_4L_4$. The lowest energy bands, 720 nm (13 889 cm^{-1}), 815 nm (12 270 cm^{-1}), 770 nm (12 987 cm^{-1}), and 870 nm (11 494 cm^{-1}) for **1**, **2**, **3**, and **5**, respectively, are assigned to the $\delta_{xy} \rightarrow \delta_{xy}^*$ transition. This band displays a clear sensitivity to the nature of the halogen ligands, and the energy of this band is red-shifted as the halogen ligands are changed from Cl to Br. Specifically, the red-shift of the racemic diastereomers is 902 cm^{-1}, and that of the meso ones is 776 cm^{-1}. These shifts are somewhat larger than those previously reported[4b] for the $Mo_2X_4(PMe_3)_4$ (X = Cl, Br) compounds, in which the torsional angles are 0°, namely 520 cm^{-1}. Another feature of this band is that for the complexes with the same halogen ligands, these lowest energy bands of the meso complexes are also red-shifted, 1619 and 1493 cm^{-1} for Cl and Br compounds, respectively, compared with the corresponding bands of the racemic complexes. This lower energy in transition in the meso diastereomers is obviously

an indication of a weaker bond between the two Mo atoms since they have larger torsional angles and longer metal–metal bond distances. The higher energy transitions in the UV–vis spectra of all complexes still remain unassigned at this time due to the lack of a general trend in these bands.

$^{31}P\{^1H\}$ NMR Spectroscopy. An interesting result was obtained from the variable-temperature $^{31}P\{^1H\}$ NMR spectra of crystalline *rac*-Mo_2Cl_4(tetraphos-1) in CD_2Cl_2/CH_2Cl_2 (1:3) as shown in Figure 9. It has two broad peaks a and b, with an upfield shift for peak a and a larger downfield shift for b as temperature decreases. Thus these two peaks come closer as the temperature is lowered. For example, the chemical shift at 173K is δ 47.6 ppm ($\Delta\nu_{1/2} \approx 32$ Hz) for a and δ 40.1 ppm ($\Delta\nu_{1/2} \approx 31$ Hz) for b. At 273K, the chemical shifts are δ 48.2 ppm ($\Delta\nu_{1/2} \approx 73$ Hz) and 38.4 ppm ($\Delta\nu_{1/2} \approx 70$ Hz) for peaks a and b, respectively. No distinct peaks can be observed at temperatures higher than 300 K and no J_{P-P} coupling in this A_2B_2 system can be obtained due to the broadness of the peaks. The variable-temperature $^{31}P\{^1H\}$ NMR spectra of the crystalline sample of *rac*-Mo_2Br_4(tetraphos-1) are very similar to the spectra of its chloride analogue. A detailed explanation for this temperature-dependent shift and broadness of the peaks is not evident at this stage. No doubt one important factor is the temperature dependent paramagnetism of this system due to a smaller singlet–triplet gap [$^1(\delta)^2 \rightarrow {}^3(\delta\delta^*)$] as the molecule twists along the Mo–Mo axis. Other factors may be the magnetic anisotropy and possible low-energy fluxional processes in this system.

For the meso diastereomers of Mo_2X_4(tetraphos-1), no peaks can be observed at room temperature, and only very broad peaks are observed at approximately 32 and 42 ppm at 178 K. We have also found that the complex *rac*-$Mo\overset{4}{-}MoCl_4(PEt_3)$ (η^3-tetraphos-2) with an average torsional angle of 11.7° is diamagnetic.[15] This further indicates that as the torsional angle χ is increased from the average value of 18.8° in the racemic diastereomers to the average value of 30.0° in the meso ones, the energy gap between the singlet ground state and the lowest triplet state is decreased. Thus the partial paramagnetism in this system is increased to such an extent that no $^{31}P\{^1H\}$ NMR signal can be observed at room temperature in meso diastereomers. Previously, we have successfully applied the variable-temperature $^{31}P\{^1H\}$ NMR method to estimate the energy separation of a low-lying triplet state from a dimagnetic ground state in a series of quadruply bonded dimolybdenum complexes with bidentate phosphine ligands.[16] However, we are not able to conduct a similar analysis for these systems with tetraphosphine ligands due to the complexity of the spectra.

For the molecules containing the meso ligand the Λ and Δ enantiomers should be interconvertable without any bond breaking or any inversion at the phosphorus atoms. If the molecules were diamagnetic, this would presumably be observable in the NMR spectra, but because of the broadening caused by the partial paramagnetism, it is impossible to garner any information on this point.

Acknowledgment. We are grateful to the National Science Foundation for support.

Supplementary Material Available: Full lists of crystallographic data, bond distances, bond angles, torsion angles, and anisotropic thermal parameters for **1–5** and ORTEP diagrams of compounds **3** and **5** (42 pages). Ordering information is given on any current masthead page.

(15) Part 2: Cotton, F. A.; Hong, B. *Inorg. Chem.*, following paper in this issue.

(16) (a) Cotton, F. A.; Eglin, J. L.; Hong, B.; James, C. A. *J. Am. Chem. Soc.* **1992**, *114*, 4915; (b) Cotton, F. A.; Eglin, J. L.; Hong, B.; James, C. A. *Inorg. Chem.*, in press.